Nonpolar 4H-AlN grown on 4H-SiC (1(1)over-bar00) with reduced stacking fault density realized by persistent layer-by-layer growth

AUTHOR(S):

Horita, Masahiro; Kimoto, Tsunenobu; Suda, Jun

CITATION:

Horita, Masahiro ...[et al]. Nonpolar 4H-AlN grown on 4H-SiC (1(1)over-bar00) with reduced stacking fault density realized by persistent layer-by-layer growth. APPLIED PHYSICS LETTERS 2008, 93(8): 082106.

ISSUE DATE:

2008-08-25

URL:

http://hdl.handle.net/2433/84574

APPLIED PHYSICS LETTERS **93**, 082106 (2008)

Nonpolar 4*H*-AlN grown on 4*H*-SiC $(1\bar{1}00)$ with reduced stacking fault density realized by persistent layer-by-layer growth

Masahiro Horita,[a] Tsunenobu Kimoto,[b] and Jun Suda[c]
Department of Electronic Science and Engineering, Kyoto University, Katsura Campus, Nishikyo-ku, Kyoto City, Kyoto 615-8510, Japan

(Received 6 June 2008; accepted 8 August 2008; published online 28 August 2008)

Nonpolar AlN layers were grown on 4*H*-SiC $(1\bar{1}00)$ substrates by plasma-assisted molecular-beam epitaxy. By using SiC substrates with well-formed step-and-terrace structures, stable layer-by-layer growth of 4*H*-AlN $(1\bar{1}00)$ can be realized. The layer-by-layer growth is confirmed by observations of anisotropic two-dimensional AlN islands on the grown surface as well as persistent reflection high-energy electron diffraction intensity oscillations. Cross-sectional transmission electron microscopy observations reveal that stacking fault generation during growth is suppressed and the stacking fault density is reduced to 1×10^{6} cm^{-1}. © *2008 American Institute of Physics*.
[DOI: 10.1063/1.2976559]

Group-III nitride semiconductors such as gallium nitride (GaN) and aluminum nitride (AlN) with nonpolar growth directions, $[11\bar{2}0]$ or $[1\bar{1}00]$, have attracted much attention for high-efficiency light-emitting devices due to the elimination of the unfavorable effects of built-in electric fields in heterostructures.[1] In particular, AlN and related alloys are being developed for devices emitting at deep-ultraviolet wavelength.[2] Several groups have reported nonpolar AlN growth on various substrates. Although a nonpolar AlN substrate would be the best option, AlN $(11\bar{2}0)$ or $(1\bar{1}00)$ wafers are available only in limited sizes and quantities because of the difficulties associated with AlN bulk growth.[3] Thus, to obtain nonpolar AlN, epitaxial growth is performed on foreign substrates that are available in large-size wafers. In recent years, sapphire $(1\bar{1}02)$ for AlN $(11\bar{2}0)$,[4] ZnO $(1\bar{1}00)$ for AlN $(1\bar{1}00)$,[5] and SiC for both nonpolar faces of AlN (Refs. 6 and 7) have been investigated. Nonpolar SiC is one of the best candidate substrates for nonpolar AlN because of its small lattice mismatch (~1%), high electrical and thermal conductivities, and chemical stability at the high temperatures needed for AlN growth.[8] Although both SiC and III-N materials have hexagonal structures, the stacking order of SiC (4*H*-SiC: *ABCBABCB*) is different from that of the nitrides (*ABAB*) in the thermally stable state. This structural mismatch results in the formation of high densities of defects such as stacking faults (SFs) and threading dislocations (TDs). To solve this problem, we have proposed isopolytypic growth of AlN, i.e., 4*H*-polytype AlN on 4*H*-SiC $(11\bar{2}0)$ or $(1\bar{1}00)$, which helps suppress dislocation formation and results in AlN layers with high crystalline quality.[9,10] With this approach, we have grown 4*H*-AlN $(11\bar{2}0)$ with low densities of SFs $(2\times10^{5}$ $cm^{-1})$ and TDs $(8\times10^{7}$ $cm^{-2})$.[11] However, in our previous studies of 4*H*-AlN $(1\bar{1}00)$ growth, high densities of SFs $(5\times10^{6}$ $cm^{-1})$ and TDs $(\sim10^{10}$ $cm^{-2})$ were found by transmission electron microscopy (TEM). We consider that these SFs and TDs are caused by imperfect replication of the substrate atomic stacking structure in the epilayer. One expects a layer-by-layer or step-flow growth mode to be more likely to realize perfect 4*H*-polytype replication than a three-dimensional (3D) growth mode. In 3D growth the substrate/film interfacial energy becomes relatively less important, favoring the equilibrium 2*H* structure of AlN. It is difficult to obtain an atomically flat 4*H*-SiC $(1\bar{1}00)$ surface, and substrate surface roughness prevented persistent AlN layer-by-layer growth in a previous study, where the reflection high-energy electron diffraction (RHEED) oscillations were observed only for several cycles at the start of growth.[10] In this study, we report that persistent layer-by-layer growth of 4*H*-AlN can be achieved on 4*H*-SiC $(1\bar{1}00)$ with an atomically flat surface exhibiting in clear step-and-terrace structures, and that the layer-by-layer growth of AlN on the flat surfaces leads to a reduced SF density as small as 1×10^{6} cm^{-1}.

The substrates investigated in this study are 4*H*-SiC $(1\bar{1}00)$ wafers. A HCl/H_2 gas-etching procedure is used to effectively remove polishing scratches and realize atomically flat surfaces for SiC (0001) (Ref. 12) and $(11\bar{2}0)$ (Ref. 11) substrates. However, on the SiC $(1\bar{1}00)$ faces a flat surface cannot readily be obtained by a similar gas-etching procedure. We have realized SiC $(1\bar{1}00)$ with atomically flat surfaces using chemical mechanical polishing (CMP) and a gas-etching treatment under optimized conditions.[13] Figure 1(a) shows the surface morphology of the SiC $(1\bar{1}00)$ substrate obtained following this treatment. After CMP and gas etching, the substrates were dipped into a HF solution, rinsed in de-ionized water, and loaded into a molecular-beam epitaxy (MBE) chamber. The MBE system is equipped with effusion cells for Ga and Al evaporation and a Veeco Unibulb rf plasma cell for producing active nitrogen (N^*). Prior to AlN growth, a Ga deposition and desorption process was performed *in situ* to remove residual oxygen from the SiC surface.[14] AlN growth was carried out at 750 °C under

[a]Electronic mail: horita@semicon.kuee.kyoto-u.ac.jp.
[b]Also at Photonics and Electronics Science and Engineering Center (PESEC), Kyoto University, Katsura Campus, Nishikyo-ku, Kyoto City, Kyoto 615-8510, Japan.
[c]Electronic mail: suda@kuee.kyoto-u.ac.jp.

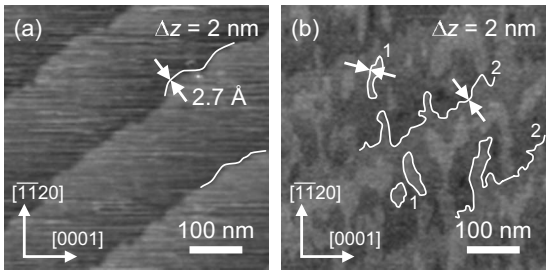

FIG. 1. AFM images of (a) a 4*H*-SiC substrate and (b) a 4-nm-(16-layer-)thick 4*H*-AlN epilayer. Pairs of arrows in both images show steps of 2.7 Å height. In (b), 2D islands (denoted by "1") and steps originating from SiC substrate steps (denoted by "2") are visible.

slightly Al-rich conditions: Al beam equivalent pressure of 8×10^{-5} Pa, N_2 flow rate of 0.75 SCCM (SCCM denotes cubic centimeter per minute at STP), and rf-plasma power of 300 W. The polytype of the AlN layers grown was confirmed to be 4*H* by *in situ* RHEED as well as high-resolution TEM (HRTEM) observations. The growth rate was typically 0.54 μm/h. The surface structures of the samples were characterized with an atomic force microscope (AFM). The crystalline quality was characterized by symmetrical and asymmetrical x-ray diffraction (XRD) rocking curves as well as TEM. TEM was performed on a JEOL JSM-2100F instrument with the field-emission electron beam accelerated at 200 keV.

The RHEED pattern along the [11$\bar{2}$0] azimuth can determine the periodicity of the (0001) stacking, i.e., distinguish between the 2*H* (wurtzite) and 4*H* structures. The periodicity of the RHEED patterns did not change with AlN growth, indicating that the AlN structure is 4*H*, which is the same structure as the 4*H*-SiC substrate. Figure 2 shows the intensity of a RHEED streak as a function of the AlN growth time. The RHEED intensity oscillated for over 100 cycles from the start of growth. The period of the oscillation corresponds to ~2.5 Å of AlN growth, calculated from post-growth thickness measurements assuming a constant growth rate. The images shown in Fig. 1(b) are the surface morphologies of a 4-nm-thick AlN epilayer. In the 4-nm-thick AlN layer, two kinds of steps were observed: one kind is steps formed from two-dimensional (2D) island edges (denoted by "1" in Fig. 1) and the other kind is vicinal surface steps with the same separation and direction as the substrate steps (denoted by "2" in Fig. 1). Both types of steps have a height of 2.7 Å, corresponding to the lattice spacing of AlN (1$\bar{1}$00) ($=\sqrt{3}a/2$). The equivalent thickness of the RHEED oscillation period (~2.5 Å) is almost the same as the lattice

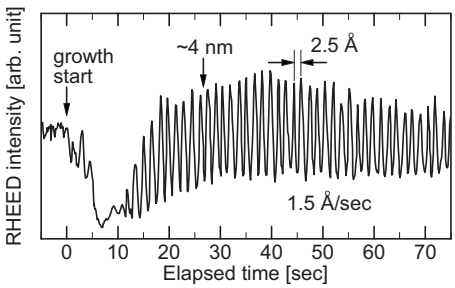

FIG. 2. Intensity of a specular RHEED diffraction streak for the (0001) azimuth as a function of AlN growth time. Oscillations continue for over 100 cycles.

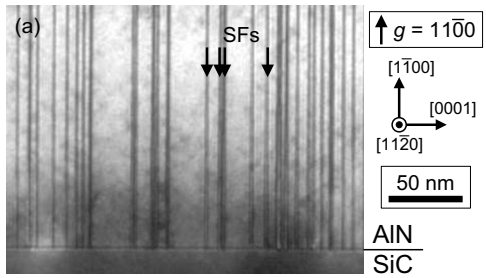

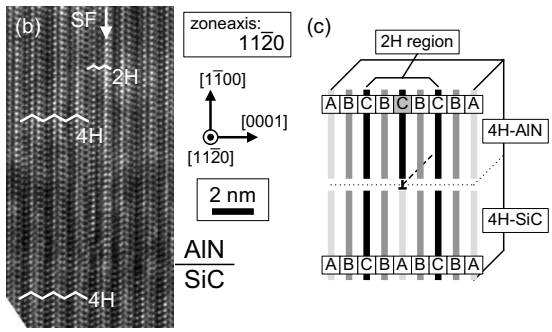

FIG. 3. Cross-sectional TEM images of a 4*H*-AlN/4*H*-SiC interface under (a) low-magnification and (b) high-resolution conditions. A schematic of the SF structure is shown in (c).

spacing of AlN (1$\bar{1}$00) (2.7 Å). Thus the AlN layer grows mainly in a layer-by-layer mode. The 2D islands of AlN in Fig. 1(b) have anisotropic shapes elongated along [11$\bar{2}$0], indicating that the velocity of step advance toward [11$\bar{2}$0] is larger than that toward {0001}.

XRD measurements were performed for the symmetrical and asymmetrical reflections. The values of the full-width at half-maximum (FWHM) of the symmetrical (1$\bar{1}$00) ω-scans were 45 and 54 arc sec with [11$\bar{2}$0] and {0001} incident beams, respectively. For the asymmetrical (1$\bar{1}$02) and (1$\bar{2}$10) ω-scans, the values of the FWHM were 54 and 60 arc sec, respectively. These values are similar to those of previously reported high-quality 4*H*-AlN (11$\bar{2}$0).[11]

To characterize SFs and dislocations, cross-sectional TEM observations were made. Figure 3(a) shows a low-magnification bright-field TEM image observed under the diffraction condition of $\boldsymbol{g}=1\bar{1}00$. It is inferred that the dark lines correspond to SFs parallel to (0001) because the widths of the dark lines increase as the sample is tilted toward {0001}. The SF density is estimated to be 1×10^6 cm^{-1}, which is much reduced compared with that of the previous study (5×10^6 cm^{-1}).[10] It is notable that almost all the SFs originate from the AlN/SiC interface in the image of Fig. 3(a). This is in contrast to the pervious work where SFs were found to have been generated not only at the interface, but also during growth of the AlN layer.[10]

To determine the detail structure of the SFs, HRTEM observations were performed. Figure 3(b) shows a cross-sectional HRTEM image of the AlN/SiC interface where an AlN SF is included. Periodic patterns with four-layer periods along the {0001} direction, which indicates 4*H* structure, were observed in the SiC substrate and the unfaulted AlN regions. Inside the AlN SF, patterns with two-layer periodicity were observed. From this HRTEM image, one may speculate that the SF structure is as shown in Fig. 3(c), i.e., atoms at *A* sites in the 4*H* stacking (*ABCB*) are shifted to *C*

sites, and a local 2*H* structure (*CBCB*) is formed. These SFs may be caused by lateral overgrowth of AlN toward {0001}. When the $(1\bar{1}00)$ surface becomes rough or 3D growth occurs, inclusions of 2*H*-AlN can grow laterally because the 2*H* structure has a lower energy than the 4*H* structure in AlN. In the previous work, the relatively rough surfaces of the SiC substrates used (which were not treated under optimized conditions) resulted in a rough AlN growth surface. The root-mean-square (rms) roughness value of a 250-nm-thick AlN layer obtained previously was 0.9 nm. Roughness of the substrate could cause SF formation during initial nucleation of AlN, and roughness of the growing AlN surface should favor the formation of additional SFs after the nucleation stage. On the other hand, the substrates investigated in the present work have well-formed step-and-terrace structure and AlN grows in a layer-by-layer mode on these flat substrates. The rms roughness value of a 270-nm-thick AlN layer grown under a layer-by-layer mode on an optimally treated substrate is as small as 0.4 nm. It is speculated that layer-by-layer growth and flat growth surfaces lead to better replication of the 4*H* structure from subsurface layers to the growing layers and inhibit the generation of SFs during AlN growth. Although the presently achieved SF density of 1×10^{6} cm^{-1} is still rather large and may limit device applications, we believe there is a cause for optimism for possible further reductions in the SF density. The TEM observations reveal that almost all the SFs originate at the AlN/SiC interface, and the RHEED oscillations are very weak in the initial growth stage of ~15 s (about ten cycles), as seen in Fig. 2. In the earliest stage of growth, AlN grew with 3D nuclei that were observed in surface morphologies of a 2 nm (eight layer) thick AlN layer (not shown). These findings suggest that SF generation may be at least partly due to instability of the growth front at this initial stage of growth. If so, then precise control of the growth front at the initial stage (e.g., by modulating the Al and N source supplies) may lead to further reductions in SF density.

In conclusion, we have achieved persistent layer-by-layer growth of 4*H*-AlN $(1\bar{1}00)$ on 4*H*-SiC $(1\bar{1}00)$ substrates by realizing SiC substrates with well-formed step-and-terrace surface structures. The layer-by-layer growth is confirmed by persistent RHEED oscillations over 100 cycles and the observation of 2D AlN islands by AFM. Moreover, layer-by-layer growth of AlN effectively suppresses SF generation during growth.

The authors would like to thank Mr. Y. Yoshioka, Dr. N. Sasaki, and Mr. H. Kinoshita from SiXON Ltd., Japan for supplying 4*H*-SiC $(1\bar{1}00)$ substrates. This work was partly supported by the Global COE Program (C09) from the Ministry of Education, Culture, Sports, Science and Technology, Japan and Grant for Industrial Technology Research (Grant No. 04A48511d) from New Energy and Industrial Technology Development Organization, Japan.

[1] P. Waltereit, O. Brandt, A. Trampert, H. T. Grahn, J. Menniger, M. Ramsteiner, M. Reiche, and K. H. Ploog, Nature (London) **406**, 865 (2000).
[2] Y. Taniyasu, M. Kasu, and T. Makimoto, Nature (London) **441**, 325 (2006).
[3] B. M. Epelbaum, C. Seitz, A. Magerl, M. Bickermann, and A. Winnacker, J. Cryst. Growth **265**, 577 (2004).
[4] N. Okada, N. Kato, S. Sato, T. Sumii, N. Fujimoto, M. Imura, K. Balakrishnan, M. Iwaya, S. Kamiyama, H. Amano, I. Akasaki, T. Takagi, T. Noro, and A. Bandoh, J. Cryst. Growth **300**, 141 (2007).
[5] K. Ueno, A. Kobayashi, J. Ohta, H. Fujioka, H. Amanai, S. Nagao, and H. Horie, Appl. Phys. Lett. **91**, 081915 (2007).
[6] T. Akasaka, Y. Kobayashi, and T. Makimoto, Appl. Phys. Lett. **90**, 121919 (2007).
[7] N. Onojima, J. Suda, T. Kimoto, and H. Matsunami, Jpn. J. Appl. Phys., Part 2 **41**, L1348 (2002).
[8] S. Stemmer, P. Pirouz, Y. Ikuhara, and R. F. Davis, Phys. Rev. Lett. **77**, 1797 (1996).
[9] N. Onojima, J. Suda, T. Kimoto, and H. Matsunami, Appl. Phys. Lett. **83**, 5208 (2003).
[10] R. Armitage, J. Suda, and T. Kimoto, Appl. Phys. Lett. **88**, 011908 (2006).
[11] M. Horita, J. Suda, and T. Kimoto, Appl. Phys. Lett. **89**, 112117 (2006).
[12] S. Nakamura, T. Kimoto, and H. Matsunami, Appl. Phys. Lett. **76**, 3412 (2000).
[13] M. Horita, T. Kimoto, and J. Suda, Jpn. J. Appl. Phys. (to be published).
[14] N. Onojima, J. Suda, and H. Matsunami, Jpn. J. Appl. Phys., Part 2 **42**, L445 (2003).